Electron Bremsstrahlung from Neutral Atoms*

H. K. Tseng† and R. H. Pratt
Department of Physics, University of Pittsburgh, Pittsburgh, Pennsylvania 15260
(Received 17 June 1974)

The complete energy spectrum for electron bremsstrahlung has been obtained, by using a numerical calculation in partial waves with numerical potentials corresponding to neutral atoms. Sample spectra are presented for electrons of kinetic energy 50 keV incident on Au and Al. The connections between elastic electron scattering and the low-frequency region of the bremsstrahlung spectrum and between photoeffect and the high-frequency region of the bremsstrahlung spectrum are demonstrated.

Recently there has been renewed interest in electron bremsstrahlung from neutral and ionized atoms. With the continuing improvements in computer technology it has become feasible to calculate directly electron bremsstrahlung cross sections in numerical potentials. We have previously reported some scattered results[1] for incident-electron kinetic energies T_1 in the range from 5 keV to 1 MeV and for radiated photon energies k from $0.4T_1$ to $0.96T_1$; good agreement was obtained with recent experimental work.[2]

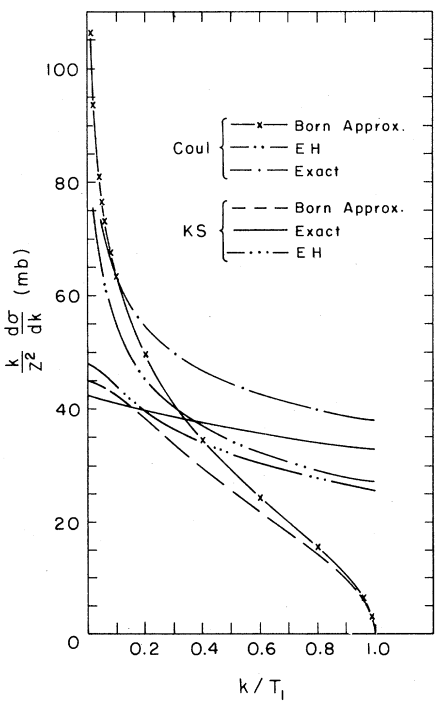

FIG. 1. Comparisons of bremsstrahlung cross sections $(k/Z^2)d\sigma/dk$ for $Z=79$, $T_1=50$ keV according to our numerical work (exact), the Born approximation (Born), and the Elwert-Haug formula (EH). Results are shown for the point Coulomb (Coul) and Kohn-Sham (KS) potentials.

We are now able to calculate the entire spectrum of k from 0 to T_1. Sample spectra for the Kohn-Sham potential[3] are shown in Figs. 1 and 2 for the bremsstrahlung from Au and Al with an incident-electron kinetic energy of 50 keV. These figures also show the point-Coulomb-potential and Born-approximation[4] predictions for the same cases.

For these energies the simplest and most widely used result is the relativistic Born-approximation calculation for a point Coulomb potential. This Bethe-Heitler formula neglects higher-order Coulomb effects and atomic-electron screening. The exact point-Coulomb result, obtained numerically, is shown in Figs. 1 and 2, as well

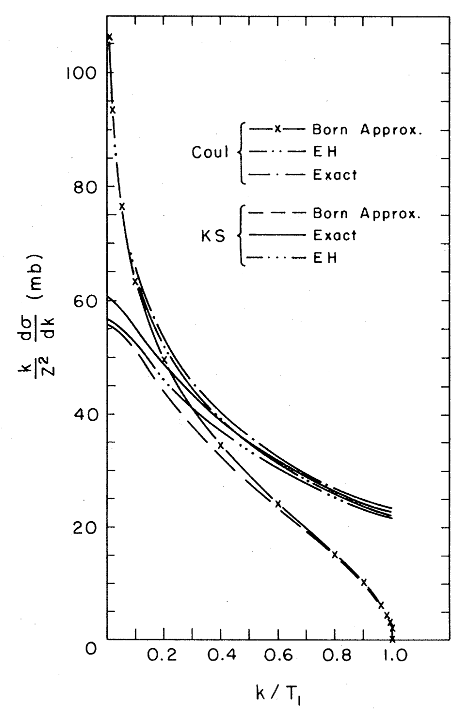

FIG. 2. Same as Fig. 1 except that $Z=13$, $T_1=50$ keV.

as an approximate analytic result due to Elwert and Haug[5] which is valid for the low-Z point-Coulomb case at all energies. In Born approximation, electron screening simply multiplies the Bethe-Heitler matrix element by a form factor; the resulting prediction for the spectrum is also shown in the figures. It is clear that none of these approximations correctly describes the spectrum. We also show the Elwert-Haug formula corrected for screening with a form factor. For the high-Z case qualitative agreement with the exact screened result is achieved, because of the cancelation of errors in the calculation of Coulomb and screening effects. For low-Z elements this approach gives quantitatively acceptable results at this energy, but its validity at lower energies remains to be determined.

In the low-frequency region of the spectrum, screening drastically reduces the cross section and removes the logarithmic divergence associated with the long-range character of the point Coulomb potential. For quantitative purposes the higher-order Coulomb effects are also of some importance and reduce the cross section further. In the high-frequency region of the spectrum, Coulomb effects increase the cross section and cause it to remain finite for $k=T_1$; for quantitative purposes the screening effects are also important and decrease the cross sections. Similar features are observed as T_1 and Z are varied. The effect of screening is adequately described by a form factor only when the Born approximation is satisfactory. Nonrelativistic results[6] are reached rather slowly.

In the low-frequency region of the spectrum, as discussed by Low,[7] the bremsstrahlung matrix element is proportional to the matrix element for elastic electron scattering. This leads to the prediction for the spectrum limit point ($k=0$)

$$\left(\frac{k}{Z^2}\frac{d\sigma_{\rm brem}}{dk}\right)_{k=0}=\frac{4\alpha}{Z^2}\int_0^\pi \sin\theta\, d\theta\left(\frac{d\sigma}{d\Omega}\right)_{\rm elas}\left[A(A^2-B^2)^{-1/2}\cosh^{-1}(A/B)-1\right],$$

where $\beta=p_1/E_1$, $A=1-\beta^2\cos\theta$, $B=1-\beta^2$, with θ the electron scattering angle. Using Lin's elastic scattering data[8] we obtain a value of the spectrum limit point for $Z=79$ of 41.7 mb at $T_1=50$ keV, in good agreement with our calculated value of 42.4 mb. Similar agreement is obtained for $T_1=100$ keV. The slope of the spectrum, which according to our numerical data is nearly constant in these high-Z cases, could also be predicted if the elastic amplitude (rather than just the cross section) were available.

In the high-frequency region of the spectrum, as first noted by Fano and co-workers[9] and then extended by Pratt,[10] the bremmstrahlung cross section is proportional to the cross section for the atomic photoelectric effect, neglecting terms of relative order $(Z\alpha)^2$. Using Scofield's exact numerical photoeffect results[11] we obtain predictions for the $k=T_1$ limit point of the spectrum which agree with our numerical bremsstrahlung calculation within 20% even for high-Z elements and low kinetic energies T_1 (50 keV) if the atomic-electron scattering is either small or is estimated approximately.[12] Experimental results for the $k=T_1$ case obtained by Starek, Aiginger, and Unfried[13] for $T_1=1.84$ MeV disagree with the Elwert-Haug predictions. Our numerical calculations agree with the experiments for high Z and with the Elwert-Haug predictions for low Z.

We are performing further calculations to study the bremsstrahlung spectrum and angular distributions systematically as functions of Z and T_1. We plan to present and discuss such data subsequently.

*Work supported in part by the National Science Foundation under Grant No. GP-32798.

†Present address: Department of Physics, National Central University, Chung-Li, Taiwan (Formosa), Republic of China.

[1]H. K. Tseng and R. H. Pratt, Phys. Rev. A 1, 528 (1970), and 3, 100 (1971).

[2]H. Aiginger, Z. Phys. 197, 8 (1966), and private communication; D. H. Rester and W. E. Dance, Phys. Rev. 161, 85 (1967); D. H. Rester, N. Edmonson, and Q. Peasley, Phys. Rev. A 2, 2190 (1970); M Scheer, E. Trott, and G. Zaks, Z. Phys. 209, 68 (1968); W. Lichtenberg and M. Scheer, private communication; R. W. Kuckuck and P. J. Ebert, Phys. Rev. A 7, 456 (1973).

[3]W. Kohn and L. S. Sham, Phys. Rev. 140, A1133 (1965); D. A. Liberman, D. J. Cromer, and J. T. Waber, Comput. Phys. Commun. 2, 107 (1971).

[4]H. A. Bethe and W. Heitler, Proc. Roy. Soc. Ser. A 146, 83 (1934); F. Sauter, Ann. Phys. (Leipzig) 20, 404 (1934); G. Racah, Nuovo Cimento 11, 461, 467 (1934).

[5]G. Elwert and E. Haug, Phys. Rev. 183, 90 (1969).

[6]A. Sommerfeld, Ann. Phys. (Leipzig) 11, 257 (1931); G. Elwert, Ann. Phys. (Leipzig) 34, 178 (1939); P. Kirkpatrick and L. Wiedmann, Phys. Rev. 67, 321 (1945).

[7]F. E. Low, Phys. Rev. 110, 974 (1958).

[8]S. R. Lin, Phys. Rev. 133, A965 (1964).

[9]U. Fano, Phys. Rev. 116, 1156 (1959); K. W. McVoy and U. Fano, Phys. Rev. 116, 1168 (1959); U. Fano,

H. W. Koch, and J. W. Motz, Phys. Rev. 112, 1679 (1958).
[10]R. H. Pratt, Phys. Rev. 120, 1717 (1960).
[11]J. H. Scofield, Lawrence Livermore Laboratory Report No. UCRL-51326, 1973 (unpublished). To obtain point-Coulomb photoeffect results from Scofield's results we have used the normalization screening theory described in the recent photoeffect review by R. H. Pratt, A. Ron, and H. K. Tseng, Rev. Mod. Phys. 45, 273, 663(E) (1973).
[12]For incident-electron kinetic energies above about 10 keV the screening effects in the high-frequency region have a simple origin in changes of wave-function normalization which are observed also in high-energy photoeffect, low-energy pair production, and single-quantum pair annihilation. See for example, H. K. Tseng and R. H. Pratt, Phys. Rev. A 4, 1835 (1971), and 7, 1423 (1973).
[13]B. Starek, H. Aiginger, and E. Unfried, Phys. Lett. 39A, 151 (1972).

Lattice Location and Hyperfine Fields of Rare-Earth Ions Implanted into Iron

R. L. Cohen
Bell Laboratories, Murray Hill, New Jersey 07974

and

G. Beyer
Joint Institute for Nuclear Research, Dubna, Union of Soviet Socialist Republics

and

B. Deutch
Institute of Physics, Aarhus University, Aarhus, Denmark
(Received 18 June 1974)

We show that the implantation and anneal behavior of Gd implanted into iron is strongly affected by the process of "internal oxidation." This result is used to clear up discrepancies in earlier measurements on rare-earth ions implanted into iron.

Since the advent of the channeling technique[1] for determining the location of impurities in single crystals, a great deal of research has been performed to study the location in the lattice, and change of that location under annealing,[2] of implanted ions. Recently, such measurements have been combined with studies of the hyperfine (hf) structure of implanted ions.

Lattice location, hf fields, and annealing behavior of rare-earth (RE) ions implanted into iron have been extensively studied.[3-6] We report here new experimental results, based on the Mössbauer spectroscopy of *Fe*:Eu^{151} (Gd^{151} is the implanted species) which show that internal oxidation of the implanted Gd ions dominates the observed behavior. The chemical and metallurgical properties of the RE ions are rather similar; thus these findings can be extended to explain the results of many previous measurements performed on RE ions implanted into iron.

The conclusions from previous work on *Fe*:RE systems can be summarized as follows: (1) Channeling lattice-location measurements[3-5] show that about 60% of implanted Yb ions are substitutional in Fe, but the remaining 40% do not occupy well-defined interstitial sites. (2) Off-line time-integral perturbed angular correlation (PAC) measurements[3,4] (using radioactive Yb implanted into Fe, with the hf field measured for the Tm daughter) indicate an "average" hf field which is substantially less than would be expected for *Fe*:Tm. (3) Both the substitutional fraction (measured by backscatter experiments) and the average hf field go to essentially zero after a brief anneal at 500°C.[3,4] After the anneal, the Yb ions do not occupy well-defined sites. (4) On-line implantation PAC (IMPAC) measurements, in which hf fields of the implanted RE ions are measured within 10^{-9} sec after the ions stop, suggest that one hf field is produced by the RE ions of a given species,[6] and that the observed fields are consistent with expectations. (5) The electron relaxation rate for Tm PAC measurements (implanted *Fe*:Yb) for an annealed (500°C) source is the same as that for Yb_2O_3:Tm, and one-third that for an unannealed source.[3]

We present here the result of Mössbauer measurements on sources of Gd^{151} implanted (4×10^{14}/